JOURNAL OF COMPUTATIONAL PHYSICS 4, 279–305 (1969)

A Comparison of Two Difference Schemes Used for Numerical Weather Prediction

JOHN M. GARY

National Center for Atmospheric Research, Boulder, Colorado 80302

Received November 8, 1968

ABSTRACT

We compare two finite difference schemes which have been used for numerical weather prediction. One is based on the scheme of A. Kasahara and W. Washington, and the second on the scheme of Y. Kurihara. We compare these schemes by applying them to the shallow water equations on a hemisphere. Our conclusion is that the Kurihara scheme is more accurate provided the uniform mesh spacing suggested by Kurihara is not used. The Kurihara scheme requires twice as much time and storage for the same mesh spacing. The Kurihara scheme is much less prone to nonlinear instability

1. INTRODUCTION

The purpose of this work is the comparison of two finite difference schemes which have been used in numerical models of the atmosphere based on the primitive equations. The first is a "leapfrog" scheme based on a staggered mesh which has been used by Kasahara and Washington [4]. The second is a scheme due to Kurihara which is derived from the integral form of the hydrodynamic equations [1]. The best way to test these schemes is to apply both to the same model of the atmosphere, but this is an unreasonable programming effort. Therefore, we adopt the same simplification as Phillips and Kurihara; which is the application of these schemes to the shallow water equations on a hemisphere instead of the primitive equations [2, 3]. This report is written so that most of the conclusions should be understood upon reading only Section 1 (Introduction). In Section 4 we give a more detailed description of the difference schemes.

The shallow water equations are

$$\frac{\partial(\varphi u)}{\partial t} = -\frac{1}{\cos\theta}\left\{\frac{\partial(\varphi u^2)}{\partial\lambda} + \frac{\partial(uv\varphi\cos\theta)}{\partial\theta}\right\} - \frac{C_h}{\cos\theta}\frac{\partial(\tfrac{1}{2}\varphi^2)}{\partial\lambda} + (C_f\sin\theta + u\tan\theta)\,v\varphi + C_d\nabla^2(\varphi u), \tag{1}$$

581/4/3-1

$$\frac{\partial(\varphi v)}{\partial t} = -\frac{1}{\cos\theta}\left\{\frac{\partial(\varphi uv)}{\partial\lambda} + \frac{\partial(\varphi v^2\cos\theta)}{\partial\theta}\right\} - C_h\frac{\partial(\frac{1}{2}\varphi^2)}{\partial\theta}$$
$$- (C_f\sin\theta + u\tan\theta)\,u\varphi + C_d\nabla^2(\varphi v), \tag{2}$$

$$\frac{\partial\varphi}{\partial t} = -\frac{1}{\cos\theta}\left\{\frac{\partial(\varphi u)}{\partial\lambda} + \frac{\partial(\varphi v\cos\theta)}{\partial\theta}\right\} + C_{d\varphi}\nabla^2\varphi, \tag{3}$$

where u, v, φ have been rendered dimensionless by use of the quantities U_0 and φ_0. The constants are defined by

$$C_h = \varphi_0/U_0^2, \qquad C_f = 2\Omega a/U_0, \qquad C_d = \sigma/aU_0, \qquad C_{d\varphi} = \epsilon_\varphi C_d$$

where Ω is the angular velocity of the earth and a is its radius. The diffusion terms (i.e., $C_d\nabla^2(\varphi u)$) are of course not part of the shallow water equations. These terms are added to eliminate nonlinear instability ([8], p.126). The diffusion coefficient σ must be taken large enough to eliminate nonlinear instability (for the centered scheme $\sigma \geqslant 4 \times 10^5$ m^2/sec). The parameter ϵ_φ allows the diffusion used for the height field to differ from that used in the momentum equations.

The range in latitude is $0 \leqslant \theta \leqslant \pi/2$ and we require the flow to be periodic in λ with period π, thus $0 \leqslant \lambda \leqslant \pi$ is the range in longitude. We require symmetry at $\theta = 0$. In the programs we set $u = v = 0$ and compute φ at the pole ($\theta = \pi/2$). Actually u and v are not defined at the pole.

In Section 4 we will describe the difference schemes as applied to the shallow water equations. To simplify matters we will here describe the difference schemes as they would be applied to the equation

$$\frac{\partial u}{\partial t} = \frac{\partial(u^2)}{\partial x} + \frac{\partial(u^2)}{\partial y} \tag{4}$$

defined for rectangular coordinates. The centered scheme is defined on the staggered mesh as shown in Fig. 1. The mesh points marked • carry values of u at the nth

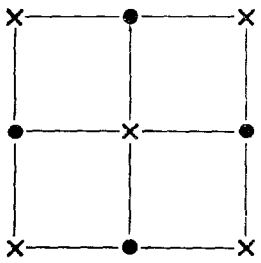

FIG. 1. Centered scheme mesh.

time level, and the × points carry values at the $(n-1)$ time level. To find values on the $(n+1)$ time level we use the following finite difference version of Eq. (4),

$$u_{i,j}^{n+1} = u_{i,j}^{n-1} + 2\,\Delta t \left\{ \frac{(u_{i+1,j}^{n})^2 - (u_{i-1,j}^{n})^2}{2\,\Delta x} + \frac{(u_{i,j+1}^{n})^2 - (u_{i,j-1}^{n})^2}{2\,\Delta y} \right\}. \tag{5}$$

Note that $u_{i,j}^{n-1}$ is computed at the × points only.

The Kurihara scheme is based on the integral form of Eq. (4),

$$\frac{\partial}{\partial t}\left\{ \int_{\Sigma_0} u\,dx\,dy \right\} = \int_{S_1} u^2\,dy - \int_{S_3} u^2\,dy + \int_{S_4} u^2\,dx - \int_{S_2} u^2\,dx \tag{6}$$

where the area Σ_0 and line segments S_i are defined by Fig. 2. (Note that we have used a variable mesh spacing in the x-direction.) The box Σ_0 with sides S_i is centered about the mesh point P_0. The integrals are approximated as follows:

$$\int_{S_1} u^2\,dy = \left(\frac{u_1 + u_0}{2}\right)^2 A_1, \tag{7}$$

$$\int_{S_2} u^2\,dx = \left(\frac{u_5 + u_0}{2}\right)^2 A_5 + \left(\frac{u_6 + u_0}{2}\right)^2 A_6, \tag{8}$$

$$\int u\,dx\,dy = u_0 V_0, \tag{9}$$

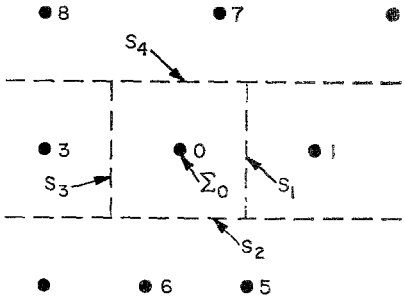

FIG. 2. Kurihara mesh.

where A_i are the lengths of the line segments indicated in Fig. 3 and V_0 is the area of the box. All the boxes are centered about the mesh point they contain.

The Kurihara scheme is quasi-conservative. This is the reason for using the above integral form of the equations. By quasi-conservative we mean that the system

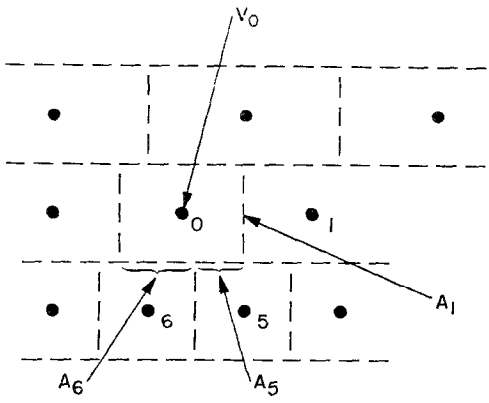

FIG. 3. Kurihara mesh.

of ordinary differential equations obtained by using only spatial difference operators on the partial differential equations conserves energy (see Section 4).

The time derivative $(\partial/\partial t)(\int_{\Sigma_0} u\, dx\, dy)$ is approximated by $(u_0^{n+1} - u_0^{n-1})/2\,\Delta t$ and the line integrals on the right are centered at the nth time level. Thus two time levels must be stored at each mesh point for the Kurihara scheme and only one time level for the centered scheme. Also we need compute u^{n+1} on half the mesh for the centered scheme and the entire mesh for the Kurihara scheme. These are important advantages for the centered scheme.

For both schemes there is trouble near the pole. If the same value of $\Delta\lambda$ is used on all circles of constant latitude, then the mesh points are too close near the pole. To avoid this we use fewer mesh points on the constant θ circles near the pole. In the case where $\Delta\theta = 5°$, we may use 4, 8, 16, 26, 36 points for $\theta = 85°$, 80°, 75°, 70°, 65°, respectively. On all circles below 65° there are 36 points, thus $\Delta\lambda = 5°$ on these circles. Thus we have an irregular mesh. The Kurihara scheme as described above can handle an irregular mesh without modification (except at the pole point itself). The centered scheme requires some interpolation where the mesh is irregular. Using the centered scheme (see Fig. 4) we need the values at the point marked $\otimes$ to compute a new value at P_0. These are obtained by linear interpolation using points P_5 and P_6. Both the Kurihara and centered schemes have only first-order accuracy at points where the mesh is irregular, but they have second-order accuracy where the mesh spacing is constant.

The differential equations conserve mass, that is $M = \iint \varphi \cos\theta\, d\theta\, d\lambda$ is independent of time. The Kurihara difference scheme also is conservative, that is $\Sigma\varphi^n 2\,\Delta\lambda \cos\theta \sin(\Delta\theta/2)$ is independent of n (provided the value of φ at the pole is computed properly). However, the centered scheme is not conservative because

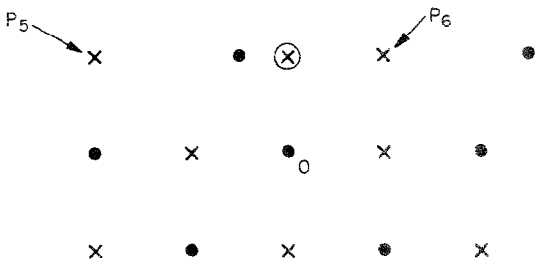

FIG. 4. Interpolation in centered mesh.

of the interpolation near the pole. The mass gain after eight days for the centered scheme at 2.8° resolution ($\Delta\theta = 2.8°$) is about .03 percent, which is probably not serious. In other cases there was a small gain or loss in mass, also not serious.

2. RESULTS

A more complete description of the results is given in NCAR Manuscript No. 68-215 [5]. In order to reduce the number of figures, we have described some results without including the relevant figures. The results are given in Figs. 5–11. The variables listed in these figures are defined in the Glossary.

The contour plots are the values of the u velocity (east-west velocity) at the time (in days) indicated on the plot. The contour interval is 10 m/sec. The maximum value of u is initially about 100 m/sec. The duration of the run (in days) is indicated by the abscissa in the lower right-hand graph.

The available energy is defined by $E_a = E - \bar{E}$ where

$$E = \iint \frac{1}{2}(u^2 + v^2)\varphi \cos\theta \, d\theta \, d\lambda + \frac{\varphi_0}{2U_0^2} \iint \varphi^2 \cos\theta \, d\theta \, d\lambda, \tag{10}$$

$$\bar{E} = \frac{\varphi_0 \bar{\varphi}^2}{2U_0^2}, \tag{11}$$

$$\bar{\varphi} = \iint \varphi \cos\theta \, d\theta \, d\lambda. \tag{12}$$

The quantities φ_0 and U_0 are used to render the equations of motion dimensionless. The kinetic energy is defined by $\iint \frac{1}{2}(u^2 + v^2)\varphi \cos\theta \, d\theta \, d\lambda$. These energy variables, normalized to maximum value one, are plotted in the lower right-hand corner.

A. *Effect of Resolution*

In this section we will discuss the effect of resolution (i.e., mesh spacing) on the results. It is difficult to isolate the effect of resolution from that caused by the diffusion which is used to stabilize the difference scheme. The diffusion affects the flow field, so we can only hold the diffusion constant and vary the resolution and the difference scheme, then vary the diffusion at fixed resolution. We fixed the diffusion at 4×10^5 m^2/sec which is slightly above the minimum value which will stabilize the centered scheme. An approximate solution derived by Haurwitz [7] is used for the initial conditions. This is the same initial condition used by Phillips and Kurihara [6, 2]. It is described in Section 4. Note that our fields extend over half the hemisphere so that the flow corresponds to wave number 6.

Figs. 5 and 6 give results for the centered scheme. There is very little difference for either the contour plots or the energy curves between JINT = 32 and 48, so we do not include the result for the JINT = 48 case (see [5]). However, there is some difference between 18, 24, and 32 (we do not show the JINT = 24 case here;

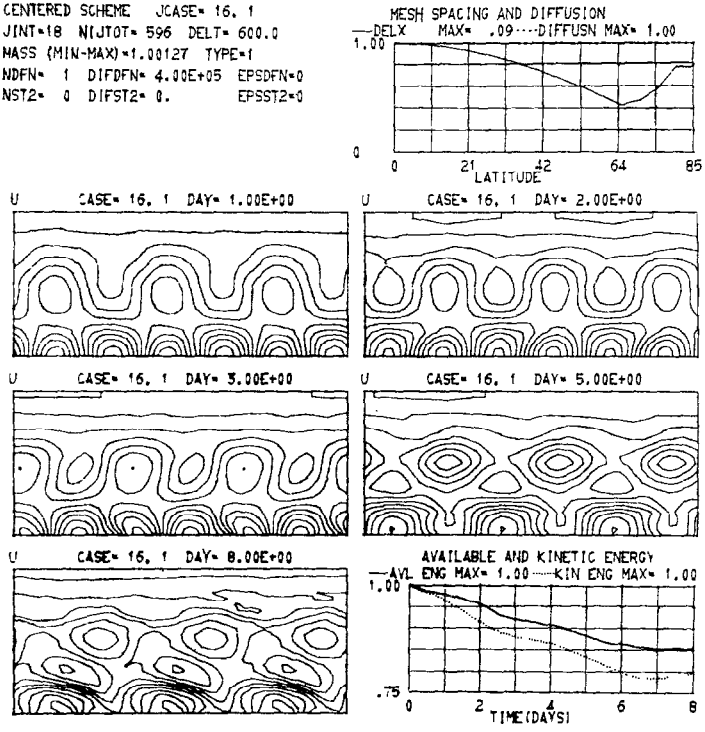

FIG. 5. Centered scheme—5° mesh.

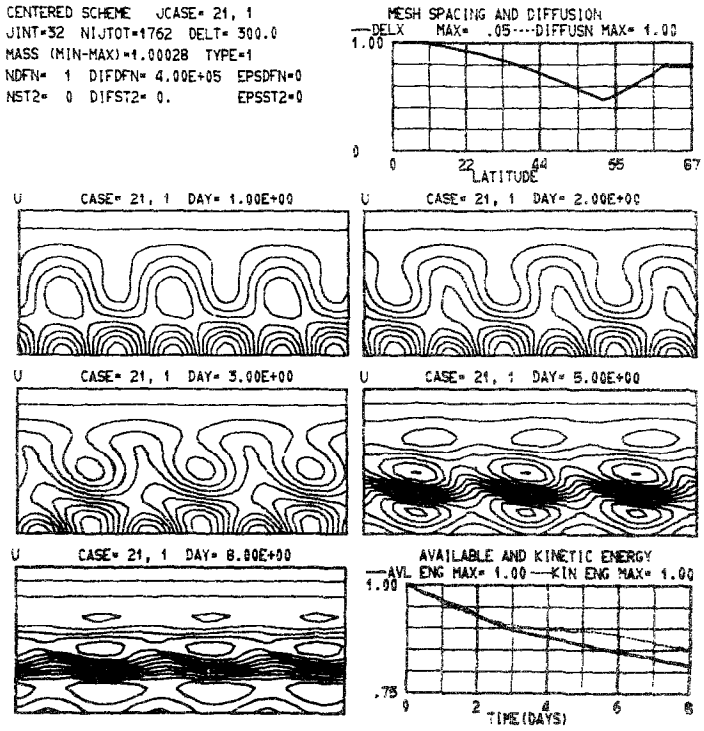

FIG. 6. Centered scheme—2.8° mesh.

see [5]). There is some difference in the velocity of the flow as measured from the movement of the flow pattern (see Table I). Note that there is no "double eye" structure for JINT = 18, thus the accuracy is not as good in this case.

TABLE I

WAVE VELOCITY—CENTERED SCHEME

$\Delta\theta$	degree/48 hours	m/sec
5°	42.5	27.8
3.75°	45.8	29.9
2.81°	46.9	30.6
1.88°	47.8	31.2

The wave velocity is obtained by measuring the horizontal movement of the high between $t = 0.0$ and $t = 2.0$ days. This high is the one centered at $\theta = 0^0$, $\lambda = 90^0$ at time zero. The approximate value obtained from the Haurwitz solution is 32.6 m/sec [6, 7]. The error in measurement from the contour plot is probably at least 1.4° or 0.9 m/sec. In addition, we have truncation error due to the difference scheme.

Figures 7–9 give the results for the Kurihara scheme. For Figs. 7 and 8 we used approximately the same mesh spacing as for the centered scheme.

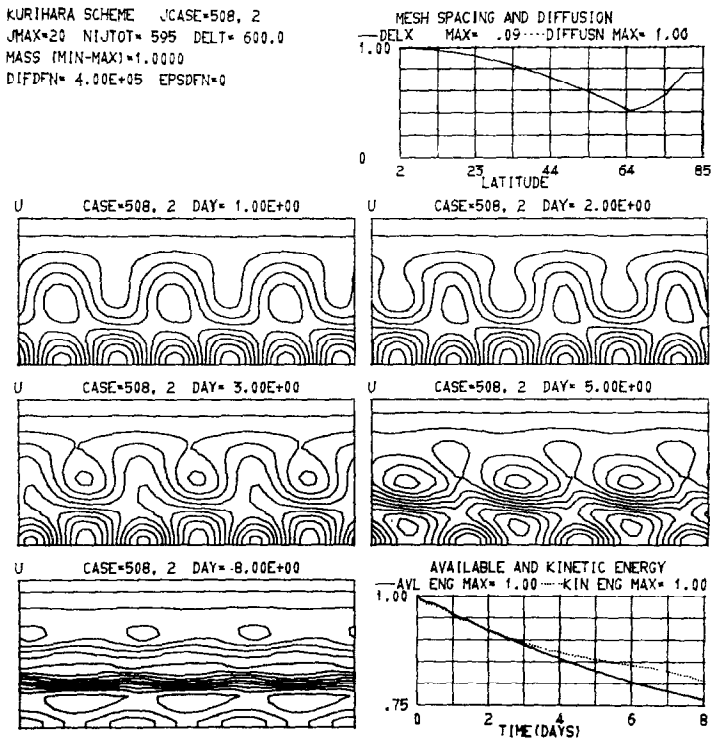

FIG. 7. Kurihara scheme—5° mesh.

For Fig. 9 we used the same mesh as Kurihara, namely we dropped two mesh points per latitude circle (four points on a 360° mesh). This has the effect of increasing the mesh spacing (Δx) toward the pole (note the upper right-hand graph in Fig. 9). The results are clearly poor for this mesh. Also, the saving in computation time for this mesh is probably not very large. The total number of points for these two meshes have the ratio 1761 : 1121. However, the Kurihara scheme for variable

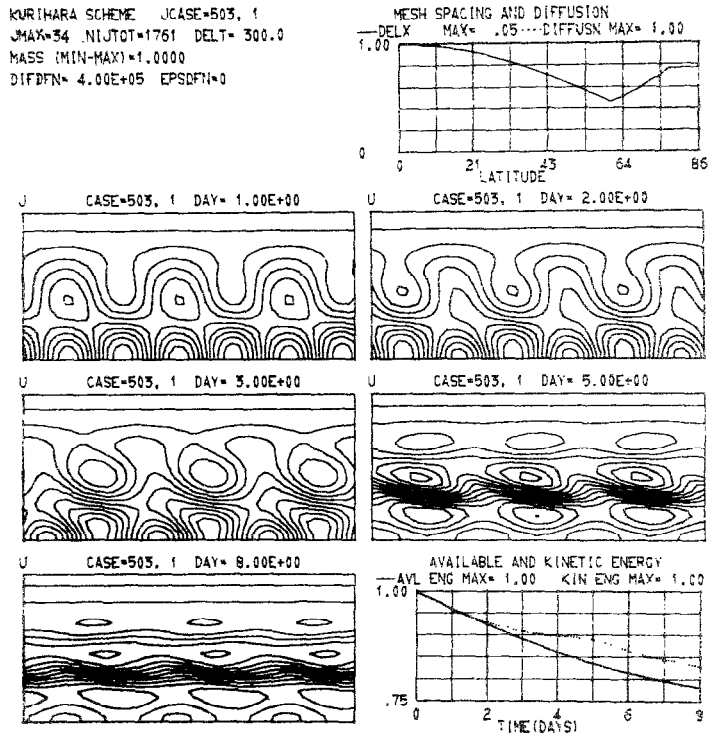

FIG. 8. Kurihara scheme—2.8° mesh.

$\Delta\lambda$ is much more complex than it is for constant $\Delta\lambda$ which reduces the difference in computing time. The superior accuracy in Fig. 8 relative to Fig. 9 probably depends on the flow fields having relatively little variation near the pole. This might not be true in a numerical model of the atmosphere.

The Kurihara scheme seems to be more accurate than the centered scheme. The Kurihara scheme at 5° seems to be slightly better than the centered scheme at 3.75° but not as good as the centered scheme at 2.81°.

B. *Effect of Dissipation*

In one case we varied the diffusion coefficient with latitude, that is, a relative variation from 1.0 at the equator to 3.75 at the pole was used. We noticed very little difference between this case and one in which the diffusion was held constant (relative value 1.0) from equator to pole.

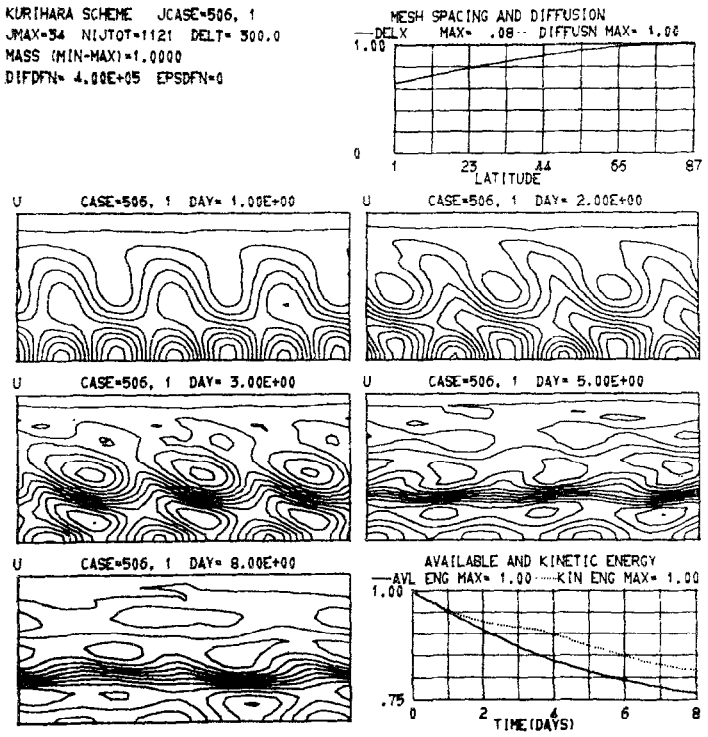

FIG. 9. Kurihara scheme—uniform mesh.

In another case a diffusion coefficient of 2×10^5 m^2/sec was used with the centered scheme. This was not sufficient to stabilize the scheme, since the computation started to explode around the seventh day. However, the qualitative pattern of the u field is the same as in Fig. 6 (where $\sigma = 4 \times 10^5$ m^2/sec) at the fifth day. A diffusion coefficient of 8×10^5 m^2/sec was also used. Again the qualitative pattern did not change, only the intensity of the field differed with σ.

In another case a slightly different type of diffusion term was used. This diffusion term is derived from the first step of the two-step Lax–Wendroff difference scheme. Consider the simple equation $u_t = u_x$. The first step of the two-step Lax–Wendroff scheme is

$$u_j^{n+1} = \frac{u_{j+1}^n + u_{j-1}^n}{2} + \frac{\Delta t}{2\,\Delta x}(u_{j+1}^n - u_{j-1}^n) \tag{13}$$

This can be written as

$$\frac{1}{2}u_j^{n+1} = \frac{1}{2}u_j^{n-1} + \frac{u_{j+1}^n + u_{j-1}^n - u_j^{n+1} - u_j^{n-1}}{2} + \frac{\Delta t}{2\,\Delta x}(u_{j+1}^n - u_{j-1}^n)$$

which becomes

$$u_j^{n+1} = u_j^{n-1} + \frac{2\,\Delta t}{2\,\Delta x}(u_{j+1}^n - u_{j-1}^n) + (u_{j+1}^n + u_{j-1}^n - u_j^{n-1} - u_j^{n+1}) \qquad (14)$$

This is the same as adding a DuFort–Frankl type of diffusion [8] with a diffusion coefficient σ such that $\Delta t\sigma/\Delta x^2 = \frac{1}{2}$ which is the maximum allowed by the stability condition for the lagged scheme. In our case of spherical coordinates there is a slight difference between the term derived from the two-step Lax–Wendroff scheme and the DuFort–Frankl term because of a variation with θ (see Section 4). In one case we used a Lax–Wendroff type of diffusion with $\sigma = 4 \times 10^3$ m^2/sec. There was little difference between this case and the DuFort–Frankl case.

For Fig. 10 we used a diffusion term of two-step Lax-Wendroff type with

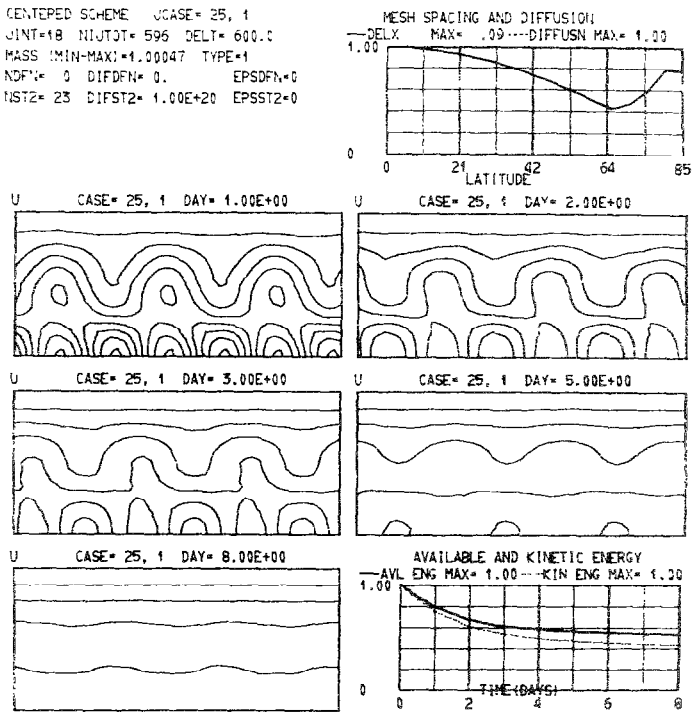

FIG. 10. Centered scheme using dissipative step every 4 hours.

$\sigma \Delta t/\Delta x^2 = \frac{1}{2}$ (the large value of DIFST 2 insures the latter). However, NST 2 = 23, which means that the Lax-Wendroff type diffusion is applied only once every 23 time steps, that is once every 3.83 hours in atmospheric time. Also, we used a 5° mesh so that Fig. 10 should be compared with Fig. 5. We include this case to show that this "two-step" type of scheme can be highly dissipative.

Next, in Fig. 11, we consider the Kurihara scheme with a reduced diffusion coefficient, $\sigma = 1 \times 10^5$ m²/sec. This should be compared with Fig. 8 where $\sigma = 4 \times 10^5$ m²/sec. The fields in Fig. 11 have the same pattern as in Fig. 8, but

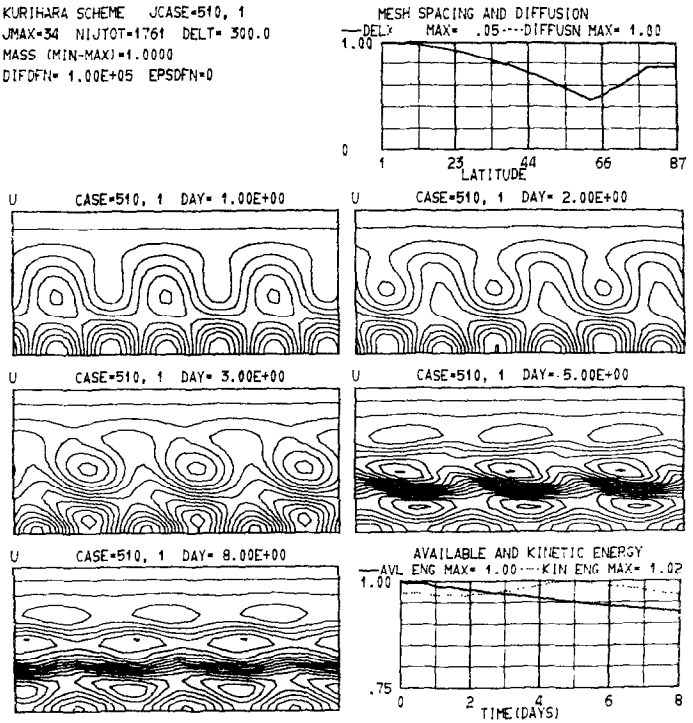

FIG. 11. Kurihara scheme—low dissipation.

they are more intense and also are not as smooth. Note that the kinetic energy is not a monotone decreasing function in this case. This case was run out to 32 days to check for instability. It was stable. The kinetic energy dropped to .85 at 32 days. With $\sigma = 0.0$ nonlinear instability develops at about 18 days with the Kurihara scheme.

In all the above cases the Coriolis term was approximated by an implicit (or time averaged) difference form, that is $\frac{1}{2}(v_{i,j}^{n+1} + v_{i,j}^{n-1})f$. In one case we used a space averaged scheme, that is $\frac{1}{4}(v_{i+1,j}^{n} + v_{i-1,j}^{n} + v_{i,j+1}^{n} + v_{i,j-1}^{n})f$. There seemed to be no essential difference.

In one case we set TYPE = 2, that is we changed the manner in which the mesh is handled near the poles (see the Glossary). This was compared with the results of Fig. 6, and there was no difference. The fact that there was no difference may be due to the nature of the test case—there is little variation near the pole.

3. Conclusions

The main conclusions can be listed as follows:

A. The Kurihara scheme is more accurate than the centered scheme for a given $\Delta\theta$. However, note that the Kurihara scheme requires twice as much storage and twice the computer time for the same value of $\Delta\theta$. Thus the Kurihara scheme at $\Delta\theta$ should be compared with the centered scheme at approximately $\Delta\theta/\sqrt{2}$.

For the centered scheme at wave number 6 we noticed little difference in accuracy out to five days between a resolution of 2.8° (32 points pole to equator) and 1.9° (48 points). There was considerable difference between 5° and 2.8° however, and

[redacted]

truncation error must be compared with other effects, such as eddy diffusion, vertical resolution, mountains, oceans, the importance of higher harmonics, etc. Thus it is difficult to draw any firm conclusions from an experiment using the shallow water equations. We only obtain an indication.

B. Kurihara used a "uniform mesh spacing" in which the number of points on a latitude circle was decreased uniformly going from the equator to the pole; that is, each circle contained two fewer points than the one below it. Thus for $\Delta\theta = 10°$, we would have 18, 16, 14,..., 2, 1 points for $\theta = 0°, 10°, 20°, \ldots, 80°, 90°$. This "uniform mesh scheme," for $\Delta\theta = 2.8°$, produced far less accurate results than one in which $\Delta\lambda$ was taken equal to $\Delta\theta$ until the $\theta \cong 65°$ circle was reached. Above $\theta \cong 65°$ the value of $\Delta\lambda$ was increased to avoid spacing the mesh points too closely.

C. The Kurihara scheme required less dissipation to eliminate nonlinear instability than did the centered scheme ($\sigma < 1 \times 10^5$ m^2/sec versus $\sigma = 4 \times 10^5$ for the centered scheme). However, the numerical models based on the primitive equations may require greater eddy diffusion for reasons that do not appear with the shallow water equations. Therefore we are not sure of the significance of this difference.

D. We tried three different types of linear diffusion terms and found little difference between them on an eight-day run. We did not try a nonlinear type of diffusion which might be more interesting.

E. We also tried two different ways of treating the Coriolis term for the centered scheme, a space average versus a time average (see Section 2). We found little difference on an eight-day run.

4. Appendix

A. *Some Integral Invariants for the Shallow Water Equations*

The shallow water equations on a sphere are given in Section 1 (θ is latitude, λ is longitude, $\theta = 0$ at the equator). Consider a rectangle R: $\theta_1 \leqslant \theta \leqslant \theta_2$, $\lambda_1 \leqslant \lambda \leqslant \lambda_2$. Let K denote the kinetic energy and P the potential energy (remember that we are using dimensionless variables), that is

$$K = \frac{1}{2}\iint_R (u^2 + v^2)\varphi \cos\theta \, d\theta \, d\lambda \tag{15}$$

$$P = \frac{C_h}{2}\iint_R \varphi^2 \cos\theta \, d\theta \, d\lambda \tag{16}$$

$$C_h = \frac{\varphi_0}{U_0^2} \tag{17}$$

Then

$$\begin{aligned}\frac{\partial K}{\partial t} = &-\frac{1}{2}\int u\varphi(u^2 + v^2)\Big|_{\lambda_1}^{\lambda_2} d\theta - \frac{1}{2}\int v\varphi(u^2 + v^2)\Big|_{\theta_1}^{\theta_2} d\lambda \\ &- C_h \iint \varphi\left(\frac{u}{\cos\theta}\frac{\partial\varphi}{\partial\lambda} + v\frac{\partial\varphi}{\partial\theta}\right)\cos\theta \, d\theta \, d\lambda \\ &+ \iint (uF_\lambda + vF_\theta)\cos\theta \, d\theta \, d\lambda\end{aligned} \tag{18}$$

and

$$\begin{aligned}\frac{\partial P}{\partial t} = &\; C_h \iint \varphi\left(\frac{u}{\cos\theta}\frac{\partial\varphi}{\partial\lambda} + v\frac{\partial\varphi}{\partial\theta}\right)\cos\theta \, d\theta \, d\lambda - C_h \int u\varphi^2\Big|_{\lambda_1}^{\lambda_2} d\theta \\ &- C_h \int v\varphi^2\Big|_{\theta_1}^{\theta_2} d\lambda + C_h \iint \varphi F_n \cos\theta \, d\theta \, d\lambda\end{aligned} \tag{19}$$

where

$$F_\lambda = C_d \nabla^2(u\varphi)$$
$$F_\theta = C_d \nabla^2(v\varphi)$$
$$F_\varphi = C_{d\varphi} \nabla^2 \varphi$$

Thus

$$\frac{\partial(K+P)}{\partial t} = -\int (C_h u\varphi^2 + \tfrac{1}{2}u\varphi(u^2+v^2))\Big|_{\lambda_1}^{\lambda_2} d\theta$$
$$- \int (C_h v\varphi^2 + \tfrac{1}{2}v\varphi(u^2+v^2)\cos\theta)\Big|_{\theta_1}^{\theta_2} d\lambda$$
$$+ \iint_R (uF_\lambda + vF_\theta + \varphi F_\varphi)\cos\theta\, d\theta\, d\lambda \tag{20}$$

We assume that the boundary conditions require u and v to vanish at the pole: φ and u to be symmetric and v skew symmetric at the equator. We consider the energy balance for the northern hemisphere, that is $\lambda_1 = 0$, $\lambda_2 = 2\pi$, $\theta_1 = 0$, $\theta_2 = \pi/2$. Also assume $F_\theta = F_\lambda = F_\varphi = 0$. Then

$$\frac{\partial(K+P)}{\partial t} = 0. \tag{21}$$

We can also show conservation of mass and angular momentum over the hemisphere, that is

$$\frac{\partial}{\partial t}\iint \varphi\cos\theta\, d\theta\, d\lambda = 0, \tag{22}$$

$$\frac{\partial}{\partial t}\iint (u + \tfrac{1}{2}C_f\cos\theta)\varphi\cos\theta^2\, d\theta\, d\lambda = 0. \tag{23}$$

The initial values are the same as those used by Phillips and Kurihara [6, 2]. The initial values of the velocity field are obtained from the following stream function

$$\psi = -a^2\omega\sin\theta + a^2K\cos^R\theta\sin\theta\cos R\lambda.$$

The height field is given by

$$\varphi = \varphi_0 + a^2A(\theta) + a^2B(\theta)\cos R\lambda + a^2C(\theta)\cos 2R\lambda$$

where

$$A(\theta) = \tfrac{1}{2}\omega(2\Omega + \omega)c^2 + \tfrac{1}{4}K^2c^{2R}[(R+1)c^2 + (2R^2 - R - 2) - 2R^2c^{-2}],$$

$$B(\theta) = \frac{2(\Omega + \omega)k}{(R+1)(R+2)}\, c^R[(R^2 + 2R + 2) - (R+1)^2 c^2],$$

$$C(\theta) = \tfrac{1}{4}K^2c^{2R}[(R+1)c^2 - (R+2)],$$

$$c = \cos\theta.$$

The values of the constants that were used are

$$\omega = K = 7.8 \times 10^{-6}\ \text{sec}^{-1},$$
$$R = 6,$$
$$\varphi_0 = 7.84 \times 10^4\ \text{m}^2/\text{sec}^2,$$
$$a = 6.37 \times 10^6\ \text{m},$$
$$\Omega = 7.29 \times 10^{-5}\ \text{sec}^{-1}.$$

Haurwitz has shown that in a nondivergent barotropic atmosphere this solution will move with angular velocity ν[7, 6].

$$\nu = \frac{R(3+R)\omega - 2\Omega}{(1+R)(2+R)}.$$

B. *The Centered Scheme*

The mesh for this scheme is laid out as follows. We define $\theta_k = (k-2)\,\Delta\theta$ where $1 \leqslant k \leqslant K$ and $\Delta\theta = \pi/2(K-2)$. The value of $K-2$ is denoted by JINT in the upper left-hand corner of output plots. On each latitude circle we place $J(k)$ equally spaced mesh points. The coordinates of these points are thus (λ_j, θ_k) where $\lambda_j = (j-1)\,\Delta\lambda_k$, $\Delta\lambda_k = \pi/J(k)$. The integer $J(k)$ is an input parameter. We require $J(k)$ to be even and non-increasing as a function of k; also we require $J(K) = 2$. Note that the domain over which we are integrating the equations is $0 \leqslant \theta \leqslant \pi/2$, $0 \leqslant \lambda \leqslant \pi$. The boundary conditions require $u(\lambda + \pi, \theta, t) = u(\lambda, \theta, t)$ and similarly for v and φ. At the pole $\theta = \pi/2$ we require $u = v = 0$. We require u and φ to be symmetric about $\theta = 0$ and v to be skew symmetric.

The mesh is staggered in space and time. We use the notation $u_{j,k} = u(\lambda_j, \theta_k, t_n)$ where $t_n = n\,\Delta t$. The variables u, v, and φ are known for even values of the time level n at the mesh points $(j, k) = (0, 2), (2, 2), (4, 2), \ldots, (1, 3), (3, 3), \ldots, (0, 4), (2, 4), \ldots$. That is, the mesh appears as shown in Fig. 12 where the points marked × carry values at even time levels and points marked • carry points at the odd time levels.

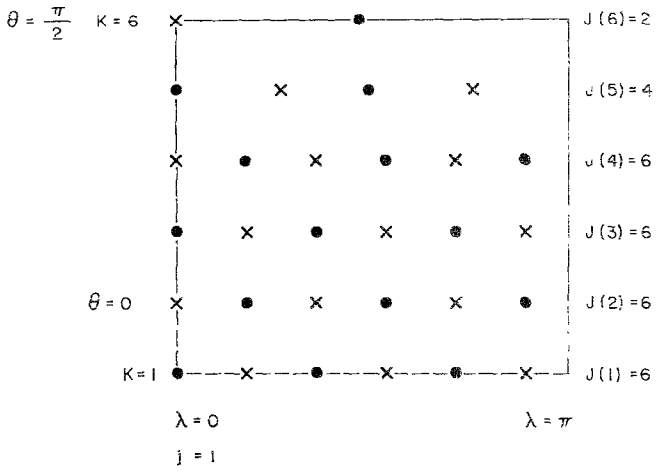

FIG. 12. Centered scheme mesh.

We will use an operator notation to describe the finite difference equations. Given a function $g_{j,k}$ defined over the mesh (λ_j, θ_k) we let

$$g_{\hat{\lambda}} = g_{j,k,\hat{\lambda}} = \frac{g_{j+1,k} - g_{j-1,k}}{2\,\Delta\lambda}, \tag{24}$$

$$g_{\hat{\theta}} = g_{j,k,\hat{\theta}} = \frac{g_{j,k+1} - g_{j,k-1}}{2\,\Delta\theta}, \tag{25}$$

$$g_A = g_{j,k,A} = \frac{g_{j+1,k} + g_{j-1,k} + g_{j,k+1} + g_{j,k-1}}{4}. \tag{26}$$

Some additional explanation is required because of irregularities in the mesh. If $j = 1$, then

$$g_{1,k,\hat{\lambda}} = \frac{g_{2,k} - g_{0,k}}{2\,\Delta\lambda}. \tag{27}$$

But $g_{0,k}$ is not defined since $j = 0$ is outside the mesh. Here we use the boundary condition which requires that all the variables be periodic in λ with period π. Thus $g_{0,k} = g_{J,k}$ where $J = J(k)$ represents the right-hand mesh point on the latitude circle $\theta = \theta_k$. Note that this requires $J(k)$ to be an even number in order that $g_{0,k}$ and $g_{J,k}$ be on the same time level. Thus

$$g_{1,k,\hat{\lambda}} = \frac{g_{2,k} - g_{J,k}}{2\,\Delta\lambda} \tag{28}$$

and

$$g_{J,k,\lambda} = \frac{g_{1,k} - g_{J-1,k}}{2\,\Delta\lambda}. \tag{29}$$

In some cases $g_{j,k,\theta}$ is not defined because of the variation in $J(k)$. For example, consider the mesh shown in Fig. 13. For the point $P = (\lambda_3, \theta_2)$ we have

$$g_{j,k,\theta} = \frac{g_{j,k+1} - g_{j,k-1}}{2\,\Delta\theta} \tag{30}$$

where $j = 3$, $k = 2$.

Since the point $(\lambda_j, \theta_{k+1})$ is not correctly positioned above (λ_j, θ_k) we must replace $g_{j,k+1}$ by an interpolated value. We used linear interpolation; that is, relative to Fig. 13 with $j = 3$ and $k = 2$,

$$g_{3,2} = \alpha g_{1,3} + (1 - \alpha)\, g_{3,3} \tag{31}$$

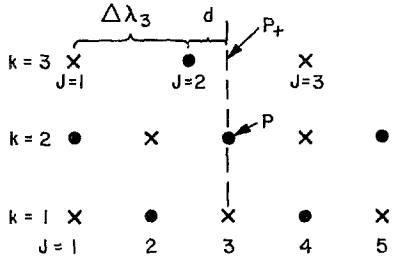

FIG. 13. Centered scheme interpolation.

where

$$\alpha = \frac{\Delta\lambda_3 + d}{2\,\Delta\lambda_3} \tag{32}$$

(Note that $d < 0$ in the case shown.)

Thus we are able to handle the variation of the mesh near the pole. If we did not increase $\Delta\lambda(k)$ near the pole, then the Courant–Friedrichs–Lewy [8] stability criterion would require a small value of Δt since the stability criterion is governed by the ratio $\Delta t/\Delta\lambda \cos\theta$.

A second method to handle the mesh variation near the pole was also tested. For this method $J(k) = J(1)$ if $k < K$ and $J(K) = 2$; that is $\Delta\lambda(k) = \Delta\lambda(1)$ for all latitude circles below the pole. We choose $J(1)$ so that $\Delta\lambda = \Delta\theta$. We then modify the spatial operator g_λ. We define a function $\Delta\gamma(k)$ such that $\Delta\gamma(k) = \Delta\theta$ below a

certain latitude (say 62°) and $\Delta\gamma(k) \cos\theta_k$ is constant above that latitude. We let $[x]$ denote the largest integer which is less than or equal to x ($x \geqslant 0$). Let $m_k = [\Delta\gamma(k)/\Delta\theta]$. Then $m_k \geqslant 1$. Let

$$\alpha = \frac{\Delta\gamma(k) - m_k \Delta\theta}{\Delta\theta} \tag{33}$$

and let

$$g^{+}_{j,k} = \alpha g_{j+m_k+1,k} + (1-\alpha)\, g_{j+m_k,k}\,, \tag{34}$$

$$g^{-}_{j,k} = \alpha g_{j-m_k-1,k} + (1-\alpha)\, g_{j-m_k,k}\,, \tag{35}$$

(that is, use linear interpolation to define $g^{\pm}_{j,k}$). Now define

$$g_{j,k,\lambda} = \frac{g^{+}_{j,k} - g^{-}_{j,k}}{2\,\Delta\gamma(k)}\,. \tag{36}$$

The value of the parameter TYPE is printed in the upper left corner of the output. If TYPE = 2, then we have used the latter definition of g_λ. If TYPE = 1, then we have used linear interpolation to define g_θ as given in Eq. (32).

We are now prepared to define the centered difference scheme. We let $g^{n}_{j,k} = g(\lambda_j, \theta_k, t_n)$ and D_u, D_v, D_φ denote the finite difference forms of the diffusion terms which we will define later. The parameter ϵ_f was in all cases zero except one for which $\epsilon_f = 1$.

$$u^{n+1}_{j,k}\varphi^{n+1}_{j,k} = u^{n-1}_{j,k}\varphi^{n-1}_{j,k} - \frac{2\,\Delta t}{\cos\theta_k}[(u^n)^2\varphi^n]_{j,k,\lambda}$$

$$- \frac{2\,\Delta t}{\ldots} [\ldots] - \frac{2\,\Delta t C_h}{\ldots} [\ldots]$$

[illegible]

$$\ldots \frac{\ldots}{\cos\theta_k} + C_f\Big)\Big\{\frac{1-\epsilon_f}{2}(v^{n-1}_{j,k}\varphi^{n+1}_{j,k} + v^{n-1}_{j,k}\varphi^{n-1}_{j,k})$$

$$+ \epsilon_f v^{n}_{j,k,A}\varphi^{n}_{j,k,A}\Big\} + D_u\,, \tag{37}$$

$$v^{n+1}_{j,k}\varphi^{n+1}_{j,k} = v^{n-1}_{j,k}\varphi^{n-1}_{j,k} - \frac{2\,\Delta t}{\cos\theta_k}[u^n v^n \varphi^n]_{j,k,\lambda}$$

$$- \frac{2\,\Delta t}{\cos\theta_k}[(v^n)^2\varphi^n\cos\theta]_{j,k,\theta} - \frac{2\,\Delta t C_h}{2\cos\theta_k}[(\varphi^n)^2]_{j,k,\theta}$$

$$- 2\,\Delta t \sin\theta_k\Big(\frac{u^{n}_{j,k,A}}{\cos\theta_k} + C_f\Big)\Big\{\frac{1-\epsilon_f}{2}(u^{n-1}_{j,k}\varphi^{n+1}_{j,k} + u^{n-1}_{j,k}\varphi^{n-1}_{j,k})$$

$$+ \epsilon_f u^{n}_{j,k,A}\varphi^{n}_{j,k,A}\Big\} + D_v\,, \tag{38}$$

$$\varphi^{n+1}_{j,k} = \varphi^{n-1}_{j,k} - \frac{2\,\Delta t}{\cos\theta_k}\{[u^n\varphi^n]_{j,k,\lambda} + [v^n\varphi^n\cos\theta]_{j,k,\theta}\} + D_\varphi\,. \tag{39}$$

To solve these equations we first determine $\varphi_{j,k}^{n+1}$, then the products $u_{j,k}^{n+1}\varphi_{j,k}^{n+1}$, $v_{j,k}^{n+1}\varphi_{j,k}^{n+1}$ and finally $u_{j,k}^{n+1}$, $v_{j,k}^{n+1}$.

The boundary conditions are used to obtain $u_{j,1}^{n+1} = u_{j,3}^{n+1}$, $\varphi_{j,1}^{n+1} = \varphi_{j,3}^{n+1}$, and $v_{j,1}^{n+1} = -v_{j,3}^{n+1}$. We use the difference scheme to compute values for $1 < k < K$. For $k = K$ (the north pole) we use $u_{j,k}^{n+1} = v_{j,k}^{n+1} = 0$. The value $\varphi_{j,K}^{n+1}$ is obtained by averaging the values of $\varphi_{j,K-1}^{n+1}$ on the first circle below the pole,

$$\varphi_{j,K}^{n+1} = \sum_{s=1}^{\frac{1}{2}J(K-1)} \varphi_{1+2s-j/\frac{1}{2}}^{n+1} \cdot J(K-1) \tag{40}$$

We will next treat the diffusion terms. We will first describe the DuFort–Frankl finite difference approximation for the Laplacian operator

$$\nabla^2 g = \frac{1}{\cos^2\theta}\frac{\partial^2 g}{\partial\lambda^2} + \frac{1}{\cos\theta}\frac{\partial}{\partial\theta}\left(\cos\theta\frac{\partial g}{\partial\theta}\right). \tag{41}$$

The term D_u in the difference scheme above is an approximation for $2\,\Delta t C_d \nabla^2(\varphi u)$ where $C_d = \sigma/aU_0$ is the dimensionless diffusion coefficient. The approximation for $\nabla^2 u$ is

$$\begin{aligned}\nabla^2 u \cong\ & \frac{1}{\Delta\lambda^2\cos^2\theta_k}(u_{j+1,k}^n + u_{j-1,k}^n - u_{j,k}^{n+1} - u_{j,k}^{n-1}) \\ & + \frac{1}{\Delta\theta^2\cos\theta_k}\left(\frac{\cos\theta_{k+1} + \cos\theta_k}{4}(2u_{j,k+1}^n - u_{j,k}^{n+1} - u_{j,k}^{n-1})\right. \\ & \left. - \frac{\cos\theta_k + \cos\theta_{k-1}}{4}(u_{j,k}^{n+1} + u_{j,k}^{n-1} - 2u_{j,k-1}^n)\right).\end{aligned} \tag{42}$$

The term D_v is $2\,\Delta t C_d \nabla^2(\varphi v)$ and D_φ is $2\,\Delta t C_d \nabla^2\varphi$.

If we set $D_u = D_v = D_\varphi = 0$ and $\epsilon_f = 1$ in the difference scheme for u, v, φ; replace the $u_{j,k}^{n-1}$, $v_{j,k}^{n-1}$ and $\theta_{j,k}^{n-1}$ terms by the averages $u_{j,k,A}^n$, $v_{j,k,A}^n$, $\varphi_{j,k,A}^n$; and then replace $2\,\Delta t$ by Δt, we obtain a finite difference scheme which is usually dissipative. This is the first step of the two-step Lax–Wendroff scheme. Another way to obtain this scheme is to set $\epsilon_f = 1$, use a centered difference approximation for the time derivative and the following formula for D_u

$$D_u = 2\,\Delta t C_d \nabla^2(\varphi u) \tag{43}$$

$$\nabla^2 u = \frac{1}{\Delta\theta^2}(u_{j+1,k}^n + u_{j-1,k}^n + u_{j,k+1}^n + u_{j,k-1}^n - 2u_{j,k}^{n+1} - 2u_{j,k}^{n-1}) \tag{44}$$

and similarly for D_v and D_φ.

The result of applying this form of the diffusion term every 23 time steps is shown in Fig. 10. This produces a rather heavy dissipation as one might expect. In these runs we have $\epsilon_f = 0$, but we still have the essence of the two-step Lax–Wendroff diffusion.

The parameter NST2 (whose value is shown on the upper left corner of the output) gives the frequency at which the two-step Lax–Wendroff type of diffusion is applied. The value of σ (units are m^2/sec) is denoted by DIFST2. If NST2 = 23, then $D_u = D_v = D_\varphi = 0$, except every 23rd time step when the diffusion terms are as given above. If NST2 = 0, then $D_u = D_v = D_\varphi = 0$ for all time steps. The value of D_φ is $C_{d\varphi}\nabla^2\varphi$ where $C_{d\varphi} = \epsilon_\varphi C_d$ and ϵ_φ is denoted by EPSST2. The values NDFN, DIFDFN, EPSDFN are similarly defined except the DuFort–Frankl type of diffusion is used.

C. *The Kurihara Scheme*

The mesh for this scheme is as shown in Fig. 14. We define $\theta_k = (k - 1.5)\,\Delta\theta$ $1 \leqslant k \leqslant K$ where $\Delta\theta = (\pi/2)/(K - 1.5)$. On each latitude circle we place $J(k)$ equally spaced mesh points. The coordinates of these points are thus (λ_j, θ_k) where $\lambda_j = (j - 1)\,\Delta\lambda_k$, $\Delta\lambda_k = \pi/J(k)$, $1 \leqslant j \leqslant J(k)$.

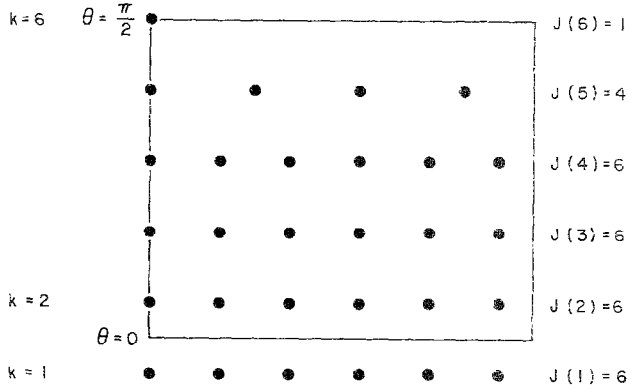

FIG. 14. Kurihara scheme mesh.

We have the same periodic boundary conditions in λ as for the centered scheme. The boundary conditions at pole and equator are also the same; namely, $u = v = 0$ at the pole, u and φ symmetric in θ, and v skew symmetric about $\theta = 0$. Again $J(k)$ is an input parameter. It is a non-increasing function of k. We require $J(K) = 1$. For reasons of program efficiency we require $\frac{1}{2}J(k) \leqslant J(k + 1) \leqslant J(k)$ and $J(1) = J(2)$. The mesh structure is shown in Fig. 14.

To derive the equations of motion we integrate the equations of motion over the "box" shown in Fig. 15. The mesh points are each contained in a rectangle centered about the mesh point. The points whose boxes border on the box about P_0 (the point at (λ_j, θ_k)) are indicated by P_m. In the case shown $1 \leqslant m \leqslant 6$. We may have the maximum value of m between 4 and 7. (We assume $J(k+1) \geqslant \frac{1}{2}J(k)$.) We denote the index set for the neighbors of P_0 by L, that is $L = \{1, 2, 3, 4, 5, 6\}$ in this case. In the case shown in Fig. 16, $L = \{1, 2, 3, 4\}$. In the case shown in Fig. 17, $L = \{1, 2, 3, 4, 5, 6\}$.

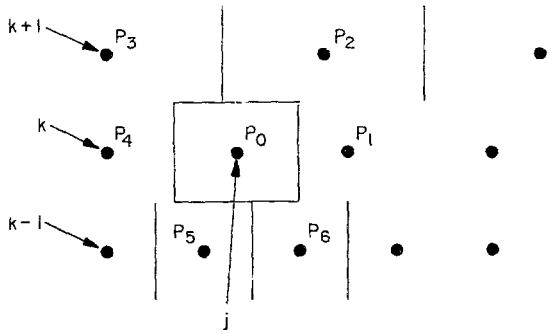

FIG. 15. Mesh point numbering—variable mesh spacing.

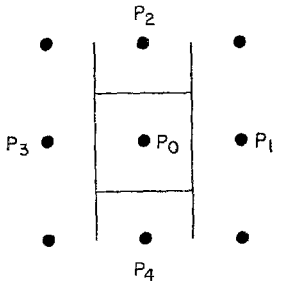

FIG. 16. Mesh point numbering—constant mesh spacing.

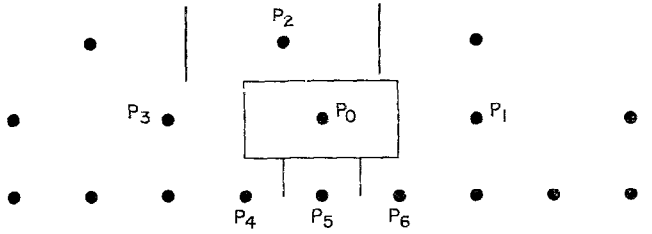

FIG. 17. Mesh point numbering—variable mesh spacing.

We denote the index set for the East-West neighbors by L_{EW} and that for the North-South by L_{NS}. Thus $L_{EW} = \{1, 4\}; \{1, 3\}; \{1, 3\}$ in Figs. 15; 16; 17, and $L_{NS} = \{2, 3, 5, 6\}; \{2, 4\}; \{2, 4, 5, 6\}$. The area of the rectangle about P_0 is $\Delta A_k = 2 \sin(\Delta\theta/2) \cos\theta_k \Delta\lambda_k$. We denote the length of the segment common to the rectangles about P_0 and P_m by S_m and $\omega_m = S_m/\Delta A_k$. Thus in Fig. 16

$$\begin{aligned} S_2 &= \Delta\lambda_k \cos\left(\theta_k + \frac{\Delta\theta}{2}\right) \\ S_4 &= -\Delta\lambda_k \cos\left(\theta_k - \frac{\Delta\theta}{2}\right). \end{aligned} \tag{45}$$

We take ω_m to be negative for the West and South sides. Using the above notation we may approximate integrals over a rectangle as given below.

$$\frac{1}{\Delta A}\iint_A \frac{\partial\psi}{\partial\lambda}\, d\lambda\, d\theta = \frac{1}{\Delta A}\int \psi\Big|_{\lambda_j-\Delta\lambda/2}^{\lambda_j+\Delta\lambda/2} d\theta \approx \sum_{L_{EW}} \left(\frac{\psi_m + \psi_0}{2}\right)\omega_m, \tag{46}$$

$$\frac{1}{\Delta A}\iint_A \frac{\partial\psi}{\partial\theta}\, d\lambda\, d\theta = \frac{1}{\Delta A}\int \psi\Big|_{\theta_k-\Delta\theta/2}^{\theta_k+\Delta\theta/2} d\lambda \approx \sum_{L_{NS}} \left(\frac{\psi_m + \psi_0}{2}\right)\omega_m. \tag{47}$$

Here ψ_m denotes the value of ψ at the mesh point P_m.

Given functions ψ, ξ defined on the mesh and the solution u, v, φ of the difference scheme we define four operators as follows:

$$\begin{aligned} D(\psi) = &\sum_{L_{EW}} \left(\frac{u_m + u_0}{2}\right)\left(\frac{\varphi_m + \varphi_0}{2}\right)\left(\frac{\psi_m + \psi_0}{2}\right)\omega_m \\ &+ \sum_{L_{NS}} \left(\frac{v_m + v_0}{2}\right)\left(\frac{\varphi_m + \varphi_0}{2}\right)\left(\frac{\psi_m + \psi_0}{2}\right)\omega_m, \end{aligned} \tag{48}$$

$$G_\lambda(\psi\xi) = \sum_{L_{EW}} \left(\frac{\psi_m\xi_m + \psi_0\xi_0}{2}\right)\omega_m, \tag{49}$$

$$G_\theta(\psi\xi) = \sum_{L_{NS}} \left(\frac{\psi_m\xi_m + \psi_0\xi_0}{2} - \psi_0\xi_0\right)\omega_m. \tag{50}$$

The above definition of G_λ is somewhat different from that given by Kurihara [1]. We use this form in order to achieve "quasi-conservation" of energy.

Next we give the difference equations, except we only difference the spatial derivatives. Thus we are considering mesh functions $\psi_{jk}(t) = \psi(\lambda_j, \theta_k, t)$ instead of

$\psi_{jk}^n = \psi(\lambda_j, \theta_k, t_n)$. This permits us to derive certain "quasi-conservative" relations. The spatial difference scheme is

$$\frac{\partial(\varphi_{jk}u_{jk})}{\partial t} = -D(u_{jk}) - C_h G_\lambda(\tfrac{1}{2}\varphi_{jk}^2) + (m_k u_{jk} + f_k)\, v_{jk}\varphi_{jk} + F_u\,, \tag{51}$$

$$\frac{\partial(\varphi_{jk}v_{jk})}{\partial t} = -D(v_{jk}) - C_h G_\theta(\tfrac{1}{2}\varphi_{jk}^2) - (m_k u_{jk} + f_k)\, u_{jk}\varphi_{jk} + F_v\,, \tag{52}$$

$$\frac{\partial \varphi_{jk}}{\partial t} = -D(1) + F_\varphi\,, \tag{53}$$

where $m_k = \tan\theta_k$ and $f_k = C_f \sin\theta_k$. This scheme is an approximation of the integral over a box of the right side of the differential equations.

The boundary conditions are $u_{j,1} = u_{j,2}$, $\varphi_{j,1} = \varphi_{j,2}$, $v_{j,1} = -v_{j,2}$ at the lower boundary. At the pole we have $u_{1,k} = v_{1,k} = 0$. The equation for $\varphi_{1,k}$ (the pole value) is

$$\frac{\partial \varphi_{1,k}}{\partial t} = -D(1) + F_\varphi\,. \tag{54}$$

Note that $\varphi_{1,k}$ has neighbors only to the South so that the operator $D(1)$ is

$$-D(1) = -\sum_{L_S}\left(\frac{v_m + v_0}{2}\right)\left(\frac{\varphi_m + \varphi_0}{2}\right)\omega_m \tag{55}$$

and ω_m is negative. The formula insures exact conservation of mass (assume $F_\varphi \equiv 0$), a property which is retained after the time derivatives are differenced.

We can prove conservation of energy for the spatial difference scheme. We first need two identities. Define an operator $\hat{D}$ by

$$\hat{D}(\psi) = \sum_{L_{EW}}\left(\frac{u_m + u_0}{2}\right)\left(\frac{\varphi_m + \varphi_0}{2}\right)\frac{\psi_m\psi_0}{2}\,\omega_m + \sum_{L_{NS}}\left(\frac{v_m + v_0}{2}\right)\left(\frac{\varphi_m + \varphi_0}{2}\right)\frac{\psi_m\psi_0}{2}\,\omega_m\,. \tag{56}$$

Then $\psi D(\psi) = (\psi^2/2)\, D(1) + \hat{D}(\psi)$. We also need

$$\sum_{j,k}\{\tfrac{1}{2}u_{jk}G_\lambda(\varphi_{jk}^2) + \tfrac{1}{2}v_{jk}G_\theta(\varphi_{jk}^2) + \varphi_{jk}D(1)\}\,\Delta A_{jk} = 0. \tag{57}$$

Here the sum is over the entire mesh.

Now if we let

$$K = \sum_{j,k}\tfrac{1}{2}(u_{jk}^2 + v_{jk}^2)\,\varphi_{jk}\,\Delta A_{jk} \tag{58}$$

and

$$P = C_P \sum_{j,k} \tfrac{1}{2}\varphi_{jk}^2 \, \Delta A_{jk} \tag{59}$$

we can show by use of the finite difference equations and the above identities that

$$\frac{\partial(K + P)}{\partial t} = 0. \tag{60}$$

(We have assumed that $F_u = F_v = F_\varphi = 0$.)

Thus this schele is "quasi-conservative" of energy. By this we mean that energy is conserved by the system of ordinary differential equations obtained when we difference the equations in space but not in time. After we difference in time the scheme is no longer conservative. If it were conservative, we would have an unconditionally stable explicit scheme for a hyperbolic system. In most cases this is impossible since it violates the Courant-Friedrichs-Lewy condition [8]. Nevertheless these "quasi-conservative" schemes tend to be less prone to nonlinear instability than the simple centered scheme.

To obtain the full finite difference scheme of Kurihara we use centered differences for the time derivatives.

$$\varphi_{jk}^{n+1} = \varphi_{jk}^{n-1} - 2\,\Delta t D(1) + D_\varphi , \tag{61}$$

$$u_{jk}^{n+1}\varphi_{jk}^{n+1} = u_{jk}^{n-1}\varphi_{jk}^{n-1} - 2\,\Delta t\{D(u_{jk}^n) + C_h G_\lambda(\tfrac{1}{2}(\varphi_{jk}^n)^2)\} + 2\,\Delta t(m_k u_{jk}^n + f_k)$$
$$\times \left[\epsilon_f v_{jk}^n \varphi_{jk}^n + (1 - \epsilon_f)\left(\frac{v_{jk}^{n+1}\varphi_{jk}^{n+1} + v_{jk}^{n-1}\varphi_{jk}^{n-1}}{2}\right)\right] + D_u , \tag{62}$$

$$v_{jk}^{n-1}\varphi_{jk}^{n-1} = v_{jk}^{n-1}\varphi_{jk}^{n-1} - 2\,\Delta t\{D(v_{jk}^n) + C_h G_\theta(\tfrac{1}{2}(\varphi_{jk}^n)^2)\} - 2\,\Delta t(m_k u_{jk}^n + f_k)$$
$$\times \left[\epsilon_f u_{jk}^n \varphi_{jk}^n + (1 - \epsilon_f)\left(\frac{u_{jk}^{n-1}\varphi_{jk}^{n+1} + u_{jk}^{n-1}\varphi_{jk}^{n-1}}{2}\right)\right] + D_v . \tag{63}$$

The diffusion terms are denoted by D_u, D_v, and D_φ and are described below. The parameter ϵ_f $(0 \leqslant \epsilon_f \leqslant 1)$ was usually set to zero. The diffusion terms are based on the DuFort-Frankl representation of the Laplacian; that is, we approximate $\nabla^2\psi$ by

$$\nabla^2\psi^n \approx \sum_{L_{\mathrm{EW}}} \frac{|\omega_m|}{\Delta\lambda_k \cos\theta_k}\psi_m{}^n + \sum_{L_{\mathrm{NS}}} \frac{|\omega_m|}{\Delta\theta}\psi_m{}^n - \sum_{L_{\mathrm{EW}}} \frac{|\omega_m|\psi_0^{n-1}}{2\,\Delta\lambda_k \cos\theta_k}$$
$$- \sum_{L_{\mathrm{NS}}} \frac{|\omega_m|}{2\,\Delta\theta}\psi_0^{n-1} - \sum_{L_{\mathrm{EW}}} \frac{|\omega_m|\psi_0^{n+1}}{2\,\Delta\lambda_k \cos\theta_k} - \sum_{L_{\mathrm{NS}}} \frac{|\omega_m|}{2\,\Delta\theta}\psi_0^{n+1}. \tag{64}$$

This is based on the form of the Laplacian

$$\nabla^2\psi = \frac{1}{\cos^2\theta}\frac{\partial^2\psi}{\partial\lambda^2} + \frac{1}{\cos\theta}\frac{\partial\left(\cos\theta\dfrac{\partial\psi}{\partial\theta}\right)}{\partial\theta}. \tag{65}$$

Then D_u, D_v, and D_φ are defined by the differenced versions of

$$D_u = 2\,\Delta t C_d \nabla^2(u\varphi), \tag{66}$$

$$D_v = 2\,\Delta t C_d \nabla^2(v\varphi), \tag{67}$$

$$D_\varphi = 2\,\Delta t C_{d\varphi} \nabla^2(\varphi). \tag{68}$$

GLOSSARY

DELT: Δt in seconds.

DELX: $\Delta x = \Delta\lambda \cos\theta$.

DIFDFN: DuFort–Frankl diffusion coefficient in m²/sec.

DIFFUSN: Multiplier to vary diffusion near the pole. The diffusion coefficient σ is multiplied by a parameter $m(\theta)$ where $m(\theta) = 1$ near the equator and may increase toward the pole. The function $m(\theta)$ = DIFFUSN is plotted with a dashed line in the upper right-hand graph. The maximum value of DIFFUSN is printed at the top of the graph.

DIFST2: Similar to DIFDFN, except for two-step diffusion.

EPSDFN: Diffusion multiplier for φ field for DuFort–Frankl case.

EPSST2: Similar to EPSDFN, except for two-step diffusion.

JCASE: Identifies the experiment.

JINT: JMAX-2.

JMAX: Number of mesh points from pole to equator, $\Delta\theta = \pi/(2*(\text{JMAX-2}))$ for centered, $\Delta\theta = \pi/(2*\text{JMAX-3})$ for Kurihara.

MASS(MIN-MAX): This is the relative loss or gain in mass at the end of the run (i.e., the mass at the end divided by the mass at the start). The mass is defined by $\sum_{ij} \varphi_{ij}\,\Delta A$, $\Delta A = 4\,\Delta\lambda \cos\theta \sin\Delta\theta$.

NDFN: Interval between application of DuFort–Frankl diffusion. Every NDFN time steps a DuFort–Frankl type diffusion (see Section 4) is applied to the u and v equations with diffusion coefficient σ = DIFDFN in m²/sec.; the value of σ used in the equation for the height field φ is EPSDFN*DIFDFN.

NIJTOT: Total number of mesh points in the region $0 \leqslant \theta \leqslant \pi/2$, $0 \leqslant \lambda \leqslant \pi$.

NST2: Similar to NDFN, except when two-step type of diffusion is used. See Section 2.B.

TYPE: The variation of the mesh near the pole is handled in one of two ways determined by the parameter TYPE. If TYPE = 1, then as the pole is approached fewer mesh points are placed on a latitude circle (i.e., a circle defined by θ = constant). Thus the value $\Delta\lambda$ increases and $\Delta x = \Delta\lambda \cos\theta$ does not become too small. The solid line in the top graph shows DELX = Δx as a function of latitude θ (the values of Δx are normalized to one). If TYPE = 2, then the same number of mesh points are placed on each latitude circle; however, the east-west derivatives are determined by an interpolation scheme which increases the effective value of Δx. That is, let $u_E(\lambda) = (1 - \alpha)\, u(\lambda + k\,\Delta\lambda) + \alpha u(\lambda + (k + 1)\,\Delta\lambda) \cong u(\lambda + \Delta x)$ and approximate $\partial u/\partial\lambda$ by $(u_E - u_W)/(2\,\Delta x)$ where $\Delta x = (k + \alpha)\,\Delta\lambda$ with $0 \leqslant \alpha \leqslant 1$. In those cases when TYPE = 2 the value of DELX, as plotted with a solid curve in the upper right-hand graph, is defined by the above equation. The maximum value of DELX is printed at the top of the graph.

C_d Diffusion term, see Section 1, paragraph 2.

$C_{d\varphi}$ Diffusion term, see Section 1, paragraph 2.

C_f Coriolis normalization, see Section 1, paragraph 2.

C_h Normalization for pressure gradient term, see Section 1, paragraph 2.

φ Geopotential.

u East-west velocity.

v North-south velocity.

References

1. Y. Kurihara and J. Holloway, *Monthly Weather Rev.* **95**, 509–530 (1967).
2. Y. Kurihara, *Monthly Weather Rev.* **93**, 399–415 (1965).
3. N. Phillips, *Monthly Weather Rev.* **87**, 333–345 (1959).
4. A. Kasahara and W. Washington, *Monthly Weather Rev.* **95**, 389–402 (1967).
5. J. Gary, A comparison of two finite difference schemes used for numerical weather prediction. NCAR Manuscript No. 68-215 (October 1968).
6. N. Phillips, Numerical integration of the primitive equations on the hemisphere. *Monthly Weather Rev.*, **87**, 333–345 (1959).
7. B. Haurwitz, "The Motion of Atmospheric Disturbances on the Spherical Earth," *J. of Marine Research*, **3**, 254–267 (1940).
8. R. Richtmyer and K. Morton, "Difference Methods for Initial Value Problems," Interscience, New York, 1967.